Additional File 2: Calibration information

Accounting for IR window transmissivity

We compared the temperatures measured by the camera to those of a blackbody calibration unit prior to deployment of each camera. The measurement was done with the camera in its enclosure, looking through the germanium infrared window (Figure AF2-1). We used a Lumasense-Mikron M310 blackbody calibration unit, which has a range of 25 to 450 °C and an effective emissivity of 1.0 at 8-14 µm. This temperature range is suitable given the 0-500 °C range of the M7500L.

We performed measurements for blackbody temperatures from 35 to 450 °C, in steps, and at each temperature step we adjusted the transmissivity correction in the camera in steps from 0.8 to 1.0 to determine a best fit correction factor. We calculated the measured temperature as the average within a field of view that occupied about half of the blackbody target surface. We discovered that the ideal transmissivity correction is temperature dependent, as shown by the example in Table AF2-1. For each camera we recorded this temperature-dependent look-up table between measured temperature at various transmissivity corrections and blackbody temperatures.

In practice, we assigned a transmissivity correction of 0.88 for the HTcam but kept the default transmissivity of 1.0 assigned to the other cameras (such as ETcam and PTcam) for the first two years of deployment. These uncorrected images still provided "ball-park" temperatures that were adequate for real-time monitoring. If and when precise temperatures were needed for research purposes, our stored calibration look-up table could then be used to convert these apparent temperatures to actual temperatures (though still not accounting for other factors affecting temperature such as fume, as described in the camera limitations section of the text).

In retrospect, we realized it would be far better to assign a lower transmissivity correction, such as 0.83, as this would extend the upper calibration temperature (see Table AF2-1). We have recently applied this change to our acquisition scheme, changing the ETcam transmissivity to 0.83 and PTcam transmissivity to 0.85 and also applied the temperature-dependent corrections from the look-up table for those transmissivities in the acquisition script so that the real-time monitoring feed of images now has corrected temperatures.

The MTcam, situated at the summit of Mauna Loa at an elevation of 4170 m, often has image temperatures dipping below 0 °C. However, we mistakenly only calibrated this camera for the 0-500 °C temperature setting prior to deployment, and thus do not have a calibration table for the -40 to 120 °C temperature setting that we currently use. As a proxy, we performed a blackbody calibration for another camera at the -40 to 120 °C setting and determined that a transmissivity correction of 0.87 resulted in temperatures accurate to within 2 °C. Note that this calibration only extended from ambient temperature (25 °C) to 120 °C. To calibrate at 0 °C we imaged a block of melting ice, assuming an emissivity of 0.97, and the resulting temperatures were 2-3 °C at transmissivities of 0.85-1.0. We assumed this 0.87 transmissivity was appropriate for the MTcam based on the fact that these two cameras compared well in calibration tests using the 0-500 °C setting. Once any high temperature activity is detected, the MTcam will immediately be changed to the 0-500 °C setting.

Although we have tried to be rigorous about our calibration procedure, described above, there is still the possibility of calibration drift once the cameras are deployed in the field. The manufacturer recommends recalibration once a year, but that would be prohibitively expensive (given the six cameras we have) and disruptive for continuous observations as it would require removing the cameras for a week or more from their observation post. Instead, we plan on less frequent in-house calibration using our M310 blackbody unit. That unit can be recalibrated for $950, and we tentatively plan on recalibrating this unit every few years, and then bringing in the cameras to do the in-house recalibration at the same frequency. Given the wide range of temperatures we often monitor, roughly accurate temperatures are adequate (within, say, 10 °C would be acceptable for most monitoring purposes), and this less frequent calibration balances our accuracy needs with our limited operating budgets.

We reiterate that this intrinsic calibration correction does not account for other, extrinsic, factors affecting the measured temperature accuracy, such as volcanic fume and the mixed pixel problem, as discussed in the manuscript.

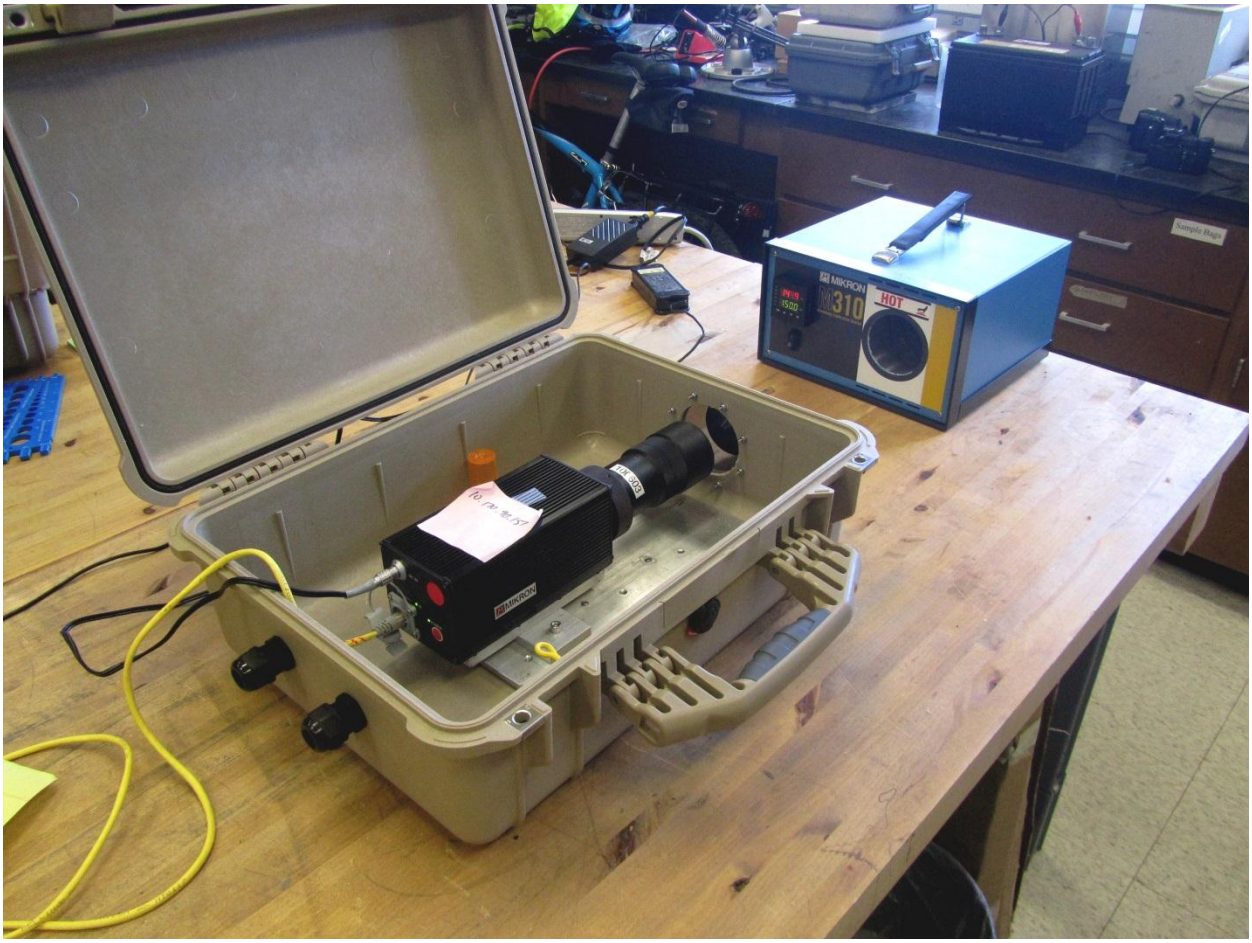

Figure AF2-1. View of calibration procedure using blackbody temperature source. The blackbody surface is inside the circular depression of the calibration unit. The camera is looking through the germanium window that is part of the enclosure.

Table AF2-1. Sample comparison between measured and blackbody temperatures (ETcam). Yellow highlighted temperatures bracket the blackbody temperature.

Blackbody temp. C	Measured temp. (Celsius) using assumed transmissivity								
	τ=0.8	0.83	0.85	0.87	0.90	0.93	0.95	0.97	1.00
35	41.3	40.1	39.2	38.4	37.4	36.2	35.5	35.0	33.9
50	56.6	55.1	54.1	53.1	51.7	50.4	49.5	48.5	47.4
75	82.5	80.4	79.0	77.6	75.6	73.8	72.5	71.3	69.6
100	107.3	104.4	102.5	100.6	98.5	96.4	95.1	93.7	91.7
150	161.3	157.3	154.7	152.1	148.6	145.2	143.1	140.9	137.8
200	212.7	208.2	205.2	202.4	198.1	194.1	191.4	189.0	185.3
250	258.8	252.6	248.8	245.0	240.6	236.4	233.7	231.0	227.0
300	309.8	302.8	298.4	294.1	287.9	282.0	278.2	274.6	269.2
350	357.8	350.0	345.0	340.2	333.4	326.8	322.6	318.5	312.7
400	404.2	395.2	389.5	384.2	376.5	369.2	364.6	360.1	353.6
450	455.7	444.3	436.9	430.1	420.3	411.9	406.4	401.4	394.2

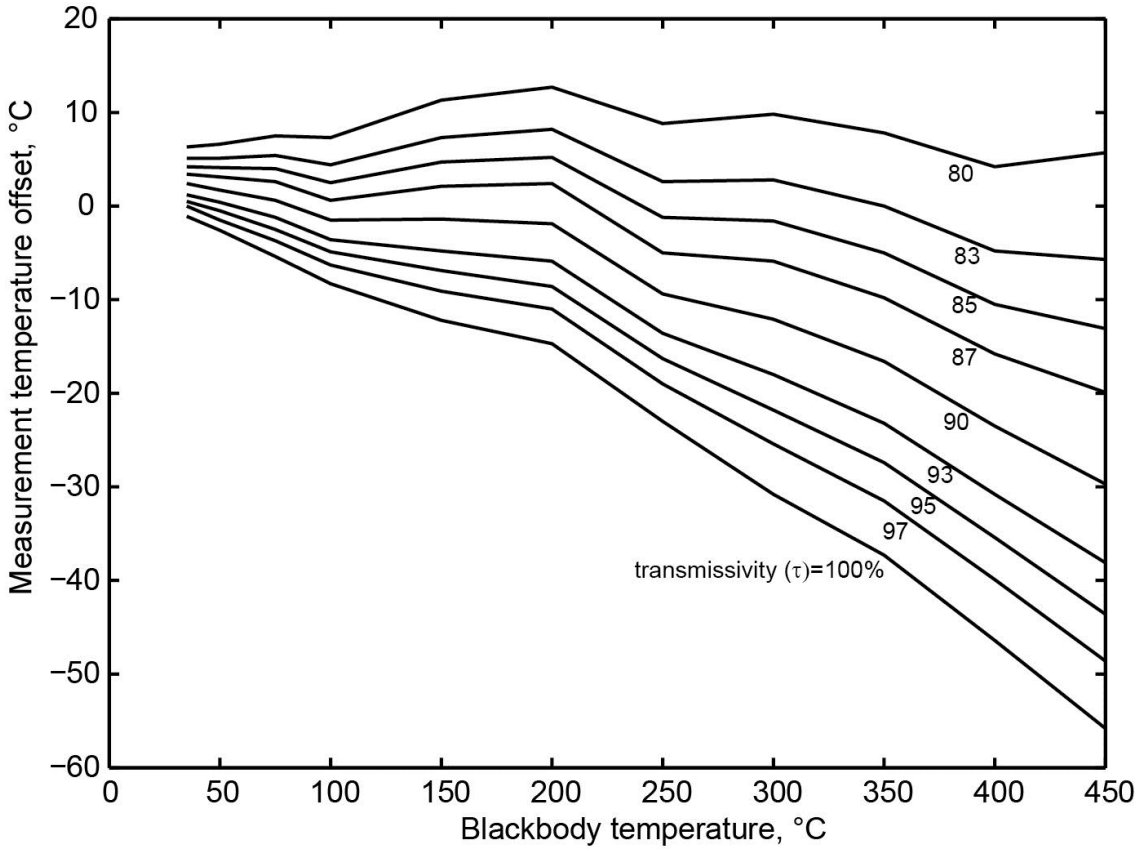

Figure AF2-2. Difference between measured and blackbody temperature for a range of transmissivity corrections for the ETcam looking through the germanium window (see Table AF2-1).

Accounting for target emissivity

Harris (2013) provides a thorough review of emissivity measurements for basalt, which tend to range between 0.90 and 0.95 in the 8-13 μm range. During the first 2-3 years of deployment the cameras were set to have a target emissivity of 1.0, but this was corrected in mid to late 2013 to 0.95.

Atmospheric effects on measured temperatures

Harris (2013) discusses the impact of atmospheric transmissivity and atmospheric radiance on the temperatures measured by thermal cameras. This effect depends on distance between the camera and target, as well as atmospheric conditions such as relative humidity. We do not account for atmospheric effects in the real-time operational images coming into the observatory, as to do so properly would complicate the acquisition process. Atmospheric effects can be simulated and applied to the images in a retrospective manner as needed (e.g. for research purposes), taking into account variations in distance within an image and changes in ambient temperature and humidity with time.

Nevertheless, for monitoring it is valuable to know the potential scale of the atmospheric effects on the measured temperatures. We follow Harris (2013) and Stevenson and Varley (2008) and use MODTRAN 5.3 (Berk et al. 2006) to model the potential impact of the atmosphere on the measured temperatures. We ran simulations for the PTcam, HTcam, and MTcam, using their respective elevations and potential viewing distances. MODTRAN results are very sensitive to relative humidity, which we show for 50-90% for the PTcam and HTcam and 20-40% for the MTcam. Other MODTRAN inputs include a standard tropical atmosphere and rural 23 km aerosol extinction. The MODTRAN results for atmospheric transmissivity and atmospheric radiance by wavelength were then weighted by the spectral response function of the M7500 camera (over the range of 7.5-13 μm), and together used to estimate the measured temperature offset due to the atmosphere. Figure AF2-3 shows that for the PTcam and HTcam, at a range of 200 m and relative humidity of 50%, the real surface temperature will be about 5% higher than the Celsius value of the apparent temperature. The real surface temperature will be about 10% higher than the Celsius value of the apparent temperature for a relative humidity of 90% and range of 200 m. Differences are greater for the MTcam, due to longer viewing distances, and are about 10-13% of the Celsius value at a distance of 3 km for relative humidity values of 20-40%, respectively.

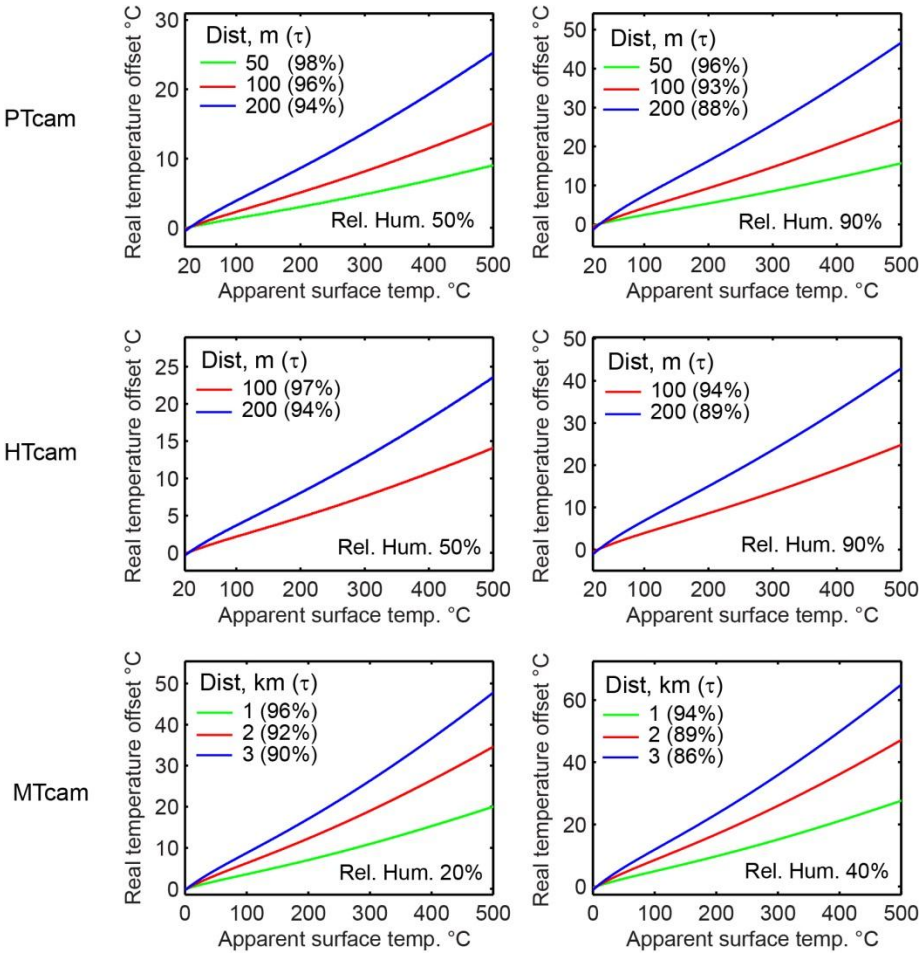

Figure AF2-3. Estimates of atmospheric effects on measured temperatures, from MODTRAN 5.3 over a range of 7.5-13 µm. The y-axis shows the difference between the measured (apparent) temperature and the real surface temperature. Over much of the range, the real surface temperature will be higher than the apparent temperature due to atmospheric attenuation of target radiance. Simulations considered varying distances between camera and target (the average atmospheric transmissivity, τ, is shown beside each distance in the legends). Rows show results for different cameras (PTcam, HTcam, MTcam), while columns show results for low (left) and high (right) relative humidity scenarios.

Effects of volcanic fume on measured temperatures

The images that we collect are also uncorrected for potentially large effects on temperature due to volcanic gases and aerosols. The PTcam and HTcam, which look into fume-filled craters, may be particularly susceptible to these effects. Sawyer and Burton (2006) showed that typical gas concentrations at Stromboli Volcano could lead to underestimates of 400 K for a surface temperature of 1200 K. The effect of the gases and aerosols will be highly variable through time, depending on the shifting of winds and activity levels. Time-synchronized FTIR (Fourier Transform Infrared spectrometer) measurements of gas concentrations along the camera viewing path would be necessary to properly account for this effect (Harris 2013).

Effects on temperature due to solar heating

Solar heating can cause significant diurnal variations in surface temperature. Figure AF2-4A shows one month of temperature values for the ETcam, for a selected portion of the image that encompasses an area of ground, several meters in front of the camera, consisting of fully cooled, inactive lava on the east flank of Puʻu ʻŌʻō cone. The mean temperature in the window has a value of around 20 °C at night, rising to 30-50 °C during the middle of the day due to solar heating. The maximum value in the window reaches almost 60 °C but is usually no more than 50 °C. For this completely inactive case, this implies that solar heating produces a diurnal variation of typically 10-30 °C. Figure AF2-4B has one month of data from the PTcam, for a selected portion of the image that encompasses an area of ground, about 100 m from the camera, consisting of recently active, but mostly cooled, lava on the crater floor that has a handful of hot cracks. The mean values are similar to those of the ETcam, being 20 °C at night and reaching to 50 °C during the middle of the day due to solar heating. The maximum values have a nighttime value (40-70 °C) significantly higher than the mean value, because the maximum values represent hot cracks on the crater floor. These maximum values reach about 80-100 °C during the middle of the day, which represents a solar heating change of about 40 °C. Therefore, for relatively low-temperature surfaces, solar heating can produce variations of 10-40 °C. Finally, we also examined a lava flow on the floor of Puʻu ʻŌʻō crater that was 2-3 days old (data not shown), and maximum temperatures (which were about 150 °C at this time) had a diurnal peak with an amplitude of 10-15 °C superimposed on the cooling curve. Together, these observations suggest that solar heating can produce diurnal variations of a few tens of degrees Celsius. This variation will be overshadowed by fluctuations in temperature on active lava surfaces (several hundreds of degrees Celsius), but is useful to recognize for monitoring low-temperature background activity.

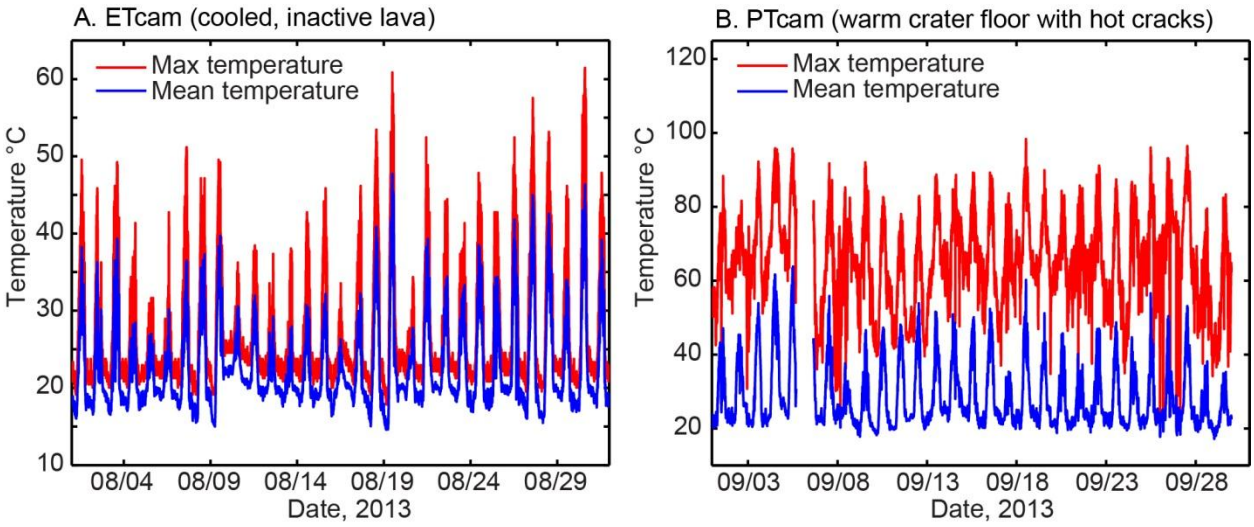

Figure AF2-4. Diurnal temperature variations due to solar heating. A) Maximum and mean temperatures in a selected portion of an image from the ETcam, showing an area of the ground close to the camera (several tens of meters away) that encompasses fully cooled, inactive lava. B) Temperatures in a selected portion of an image from the PTcam, showing an area of the ground about 100 m away from the camera that encompasses slightly warm, recently active lava flows on the crater floor of Puʻu ʻŌʻō that contain hot cracks.

Effects of mixed-temperature pixels

In many situations a hot surface may only occupy a portion of the pixel footprint, and the resulting pixel-integrated temperature is a mixture of the background and hot surface temperatures. This mixed-pixel problem is addressed in detail in Harris (2013). In Figure AF2-5 we illustrate a scenario where the background surface temperature is 20 °C, and some fraction of the pixel is occupied by a hot object. The pixel-integrated temperature is calculated based on the weighting of radiance of the two components by their respective area, over the 7.5-13 µm range. Relatively small areas of very hot surfaces can produce a large effect on the pixel-integrated temperature. For instance, a hot object at 1000 °C covering just 1% of the pixel produces a pixel-integrated temperature of almost 60 °C.

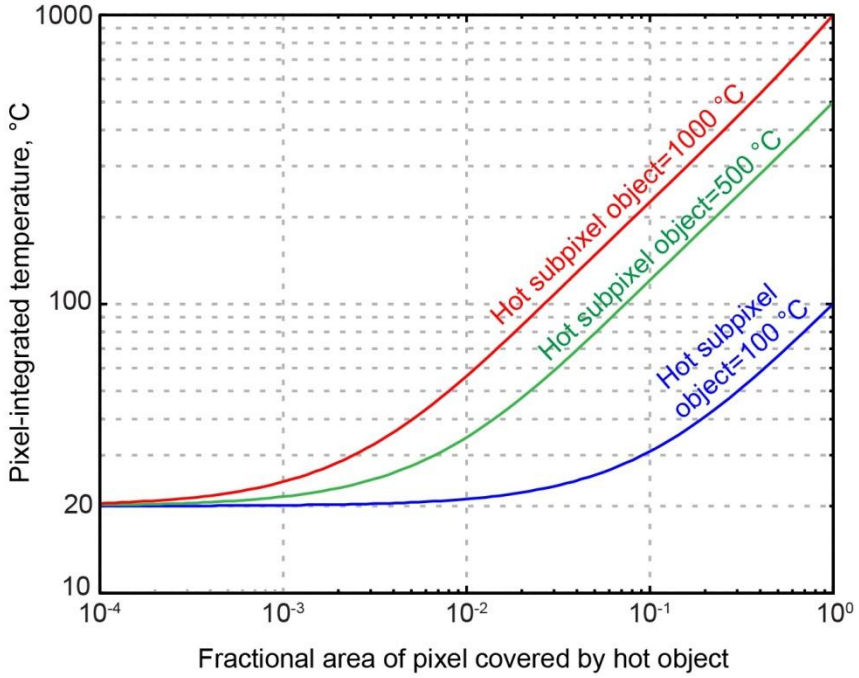

Figure AF2-5. Pixel-integrated temperature based on the fractional area of the pixel occupied by a hot object. Background temperature is assumed to be 20 °C.